Observation of Self-Amplified Spontaneous Emission and Exponential Growth at 530 nm

S. V. Milton,* E. Gluskin, S. G. Biedron, R. J. Dejus, P. K. Den Hartog, J. N. Galayda, K.-J. Kim, J. W. Lewellen, E. R. Moog, V. Sajaev, N. S. Sereno, G. Travish, N. A. Vinokurov,† N. D. Arnold, C. Benson, W. Berg, J. A. Biggs, M. Borland, J. A. Carwardine, Y.-C. Chae, G. Decker, B. N. Deriy, M. J. Erdmann, H. Friedsam, C. Gold, A. E. Grelick, M. W. Hahne, K. C. Harkay, Z. Huang, E. S. Lessner, R. M. Lill, A. H. Lumpkin, O. A. Makarov, G. M. Markovich, D. Meyer, A. Nassiri, J. R. Noonan, S. J. Pasky, G. Pile, T. L. Smith, R. Soliday, B. J. Tieman, E. M. Trakhtenberg, G. F. Trento, I. B. Vasserman, D. R. Walters, X. J. Wang,‡ G. Wiemerslage, S. Xu, and B.-X. Yang

Advanced Photon Source, Argonne National Laboratory, Argonne, Illinois 60439
(Received 21 March 2000)

Experimental evidence for self-amplified spontaneous emission (SASE) at 530 nm is reported. The measurements were made at the low-energy undulator test line facility at the Advanced Photon Source, Argonne National Laboratory. The experimental setup and details of the experimental results are presented, as well as preliminary analysis. This experiment extends to shorter wavelengths the operational knowledge of a linac-based SASE free-electron laser and explicitly shows the predicted exponential growth in intensity of the optical pulse as a function of length along the undulator.

Synchrotron radiation generated by passing a high-energy electron beam through an undulator magnet is the mainstay of third-generation synchrotron light sources. In such systems, the electrons within a bunch emit incoherently. However, it is possible to generate conditions that make it favorable for the electrons to begin radiating coherently and thereby produce a large enhancement of the synchrotron radiation—the free-electron laser (FEL).

An alternative approach to FEL oscillator and amplifier configurations is to rely on self-amplified spontaneous emission (SASE) [1,2]. With SASE, conditions are set up within the beam/undulator system so that very high amplification of the beam shot noise is achieved. In SASE a favorable instability starts from the natural synchrotron radiation and develops into microbunching within the electron bunch at a scale length equal to the resonant wavelength of the undulator and beam system. Electrons within the microbunch begin to radiate coherently and enhance the microbunching, leading to an exponential increase of power as a function of distance along the undulator system. Since SASE does not require mirrors or a seed pulse it is, in principle, scalable to x-ray wavelengths. Very high SASE gain has been measured at 12 μm [3] and during the course of preparing this Letter SASE gain was also measured elsewhere at 109 nm [4]. Exponential growth of radiation intensity along the beam path has also been observed at millimeter wavelengths [5] for a system in which a waveguide provided some mitigation of diffraction effects. However, measurements and comparison to theories of the exponential growth of the signal along the undulator at visible wavelengths or shorter are needed in order to provide confidence in the design of future-generation machines based on this method.

Design reports have been written [6–9] detailing SASE-FEL-based light sources at x-ray wavelengths. SASE-mode operation requires a high-brightness (suitably dense 6D phase space) electron beam [10,11] and long, high-quality undulator systems. The low-energy undulator test line (LEUTL) system at the Advanced Photon Source (APS), Argonne National Laboratory, consisting of a high-brightness photocathode rf electron gun system coupled to the 650-MeV APS linac and a very long undulator system, is well suited to push the wavelength frontier of a SASE-FEL system. We report here on the first evidence of exponential growth of the optical signal, SASE operation, at 530 nm.

LEUTL BASIC DESCRIPTION

The LEUTL system was built as an extension of the APS linac. A photocathode rf gun system borrowed from Brookhaven National Laboratory is the source for the very high-brightness electron bunches [10,11]. This rf gun system is driven by a picosecond Nd:glass laser system [12]. A new enclosure, in line with the linac, houses the undulator system. At present there are five 2.4-m undulators and associated diagnostic systems installed. A more complete description of the LEUTL system can be found elsewhere [13–17]. Here we will describe the undulator and diagnostics systems.

The undulator system is built of identical cells. Each cell contains a fixed-gap 2.4-m-long undulator with a 3.3-cm period and a K value of 3.1. There is a diagnostic station, a horizontal focusing quadrupole, and horizontal and vertical steering between each of the five undulators. The longitudinal spacing is set to ensure proper phase matching of the optical fields at successive undulator sections.

Figure 1 is a representative diagram of the diagnostics station. Electron beam diagnostics include yttrium aluminum garnet (YAG) and optical transition radiation (OTR) screens viewed by a charge coupled device (CCD) camera. Two sets of filter wheels afford both intensity and
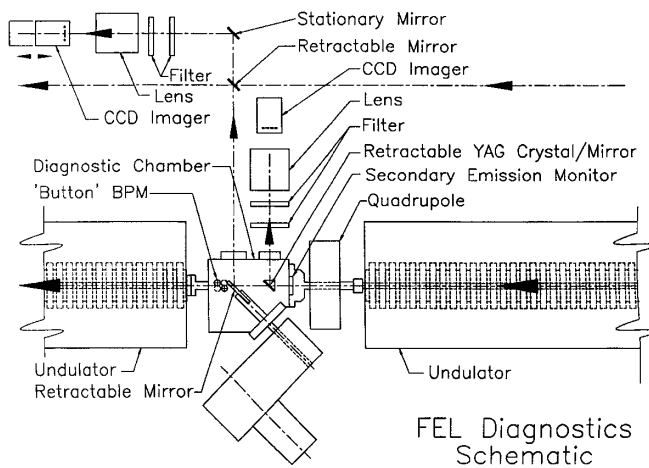
FIG. 1. Schematic of an FEL diagnostics station.

wavelength selectivity. Completing the primary electron beam diagnostics at each station are capacitive pickup beam position monitors (BPMs).

Our primary visible light detectors (VLDs) consist of additional three-position actuators. These are used to deflect the generated light through a set of filters to a separate digital CCD camera. The actuator holds an aluminized mirror. The three positions are (1) out, (2) mirror, and (3) mirror with 600-μm hole. All five mirror hole centers have been aligned along the beam line to within 20 μm of the ideal electron beam trajectory. The cameras viewing these mirrors are on translation stages and the lenses are fixed. This allows the cameras to be focused at the mirror, at infinity, or at any distance in between. Focus at infinity allows one to view the angular distribution of the optical radiation.

At the entry to the undulator system is a green alignment laser system. It is used to ensure that all mirrors are positioned and angled correctly. It also serves as a calibration source for the optical systems.

MEASURED ELECTRON BEAM PROPERTIES

Current distribution.—(i) Charge: Beam charge is measured with calibrated integrating current toroids (ICTs) coupled to gated integrators. There are three ICTs along the system: one immediately following the photocathode rf gun, a second just upstream of the undulator system, and a third following the undulator system. (ii) Bunch Length: The electron bunch length at the end of the linac is measured in three different ways. The most direct way is by observing with a streak camera the light from an OTR screen [18]. A second measure is obtained by phasing an accelerating section such that the beam traverses it at the zero crossing point of the rf field. The induced energy spread is correlated to the bunch length (through dispersion), and the beam is observed on a fluorescent screen following a spectrometer dipole magnet. The final method is to use the spectral distribution of the radiation emitted from the beam as it passes through the undulator system [19].

Typical values for bunch lengths are shown in Table I. Bunch-length variations occur due to different machine and drive laser tunings, as well as space-charge effects. The bunch length measured during this experiment was approximately 5 ps FWHM. Bunch shapes are assumed Gaussian; however, the details of the distribution are not entirely essential to this Letter, as it is the peak of the distribution that exhibits the largest gain and dominates the signal.

Emittance and Twiss parameters.—Following acceleration in the linac a three-screen emittance measurement system is employed to both measure the emittance and match the Twiss parameters into the transfer line. Emittance is determined by an rms fit to the beam distribution measured at the three screens. Typical values are 5π mm mrad in both planes. These are rms whole beam normalized emittances using spot-size averages of ten profile measurements at each screen. Fluctuations of the distribution are seen shot to shot. We believe most of this fluctuation is due to wakefield and structure effects along the linac, driven by slight variations in charge per bunch, and trajectory jitter. These fluctuations affect the rms emittance determination and can be quite large at times; however, with proper tuning the range of whole beam emittance measured is roughly from 4π to 8π mm mrad with the most probable value being 5π mm mrad (Table I).

An added feature of the emittance measurement is the determination of the Twiss parameters at the linac exit. Although we achieve a good match at this point, we have not measured the Twiss parameters and emittance directly at the entrance to the undulator. We believe the match is adequate into the undulator system; nevertheless, we quote a range for the average beta within the undulator of 1.2 to 3.0 m with the most probable value being 1.5 m.

Energy and energy spread.—Beam energy was determined from the deflection angle through a calibrated energy spectrometer dipole. A final adjustment of beam energy was made based on the light generated by the beam in the undulator and passed through an optical bandpass filter (530-nm center with 10-nm bandwidth).

Beam energy spread was measured by viewing the beam following the drift beyond the energy spectrometer dipole.

TABLE I. Beam parameters for 0.7-nC per bunch conditions.

	Most probable	Minimum/maximum
Beam energy	217 MeV	216 to 218 MeV (limited by the 530-nm bandpass filter)
Normalized emittance	5π mm mrad	4π to 8π mm mrad
Charge per pulse	0.7 nC	0.6 to 0.8 nC
Bunch length	5 ps FWHM	4 to 7 ps
Energy spread	$\sim$0.1%	<0.1% (spot-size limited) to 0.2%
Average beta in undulators	1.5 m	1.2 to 3.0 m

We could consistently make the whole beam energy spread observed at the end of the linac less than our present resolution of 0.1%; however, we do experience phase drift and jitter, which affects both long-term performance as well as shot-to-shot jitter.

Trajectory. — Beam trajectory through the undulators is primarily measured using the BPM system. There is one BPM located at each experimental station between undulators, as well as upstream and downstream of the undulator system. In this configuration single-pass resolution for a 1-nC electron bunch is below 10 μm. These BPMs are augmented by position determination of the visible optical transition radiation from an adjacent VLD retractable mirror. This particular mirror also has a third position with a 600-μm hole that has been surveyed and coincides with the center of the desired beam trajectory. Threading beam through this hole provides a very good confirmation of rough trajectory alignment. The beam size at these holes is roughly 150 μm rms.

OPTICAL MEASUREMENTS

Gain per undulator. — The measured integrated optical intensity along the undulator string is plotted in Fig. 2. Images of the light from 200 individual shots were collected at each of the four available VLDs along the undulator string. The measurements from different VLDs are from different shots, i.e., they are not collected simultaneously. The integrated intensity was determined for each image. In Fig. 2 the triangles show the integrated intensity for the 0.7-nC per bunch charge conditions, whereas the squares show the integrated intensity for the 0.45-nC per bunch charge conditions. Trajectory jitter through the undulators is believed to be the cause of significantly more intensity jitter than expected from predicted shot noise. The 10-nm bandpass filter centered at 530 nm was also inserted at the time of the measurements; energy jitter, therefore, also results in jitter of the intensity. Because of these sources of jitter, as yet outside of our control, we have elected to average only the top 5% of the intensity measurements at the VLDs. It is not possible, then, to assign error bars significant and meaningful to the stochastic nature of the SASE process.

Angular distribution. — The angular distribution of the optical pulse following the first and fourth undulators was also determined. The FWHM of the angular distribution of the beam after the fourth undulator, at 0.46 mrad, is smaller than that after the first undulator, 0.74 mrad. This narrowing of the angular distribution is what is expected as SASE grows to dominate the spontaneous emission and gain guiding begins (no waveguide needed). The actual narrowing in our experiment is larger than what is suggested by the measurements. This is because there was a 10-nm-wide bandpass filter, centered at 530 nm, placed in the path of the light from the first undulator, but there was no such filter for the light after the fourth undulator. This filter makes the apparent angular width significantly smaller than the actual width. The only filter following the fourth undulator was a neutral density filter that attenuates the intensity 1000 times. It was needed to prevent saturation of the CCD camera. The background due to spontaneous undulator radiation, which is broader than the SASE component, is attenuated by the neutral density filter to a level that is a factor of 5 below the noise level of our eight-bit digital cameras and so was not visible on the VLD camera following the fourth undulator.

ANALYSIS

Gain length. — In the SASE FEL, the Fourier harmonics of the beam current $I_\omega(s, z)$ at frequency ω, where s is the position along the bunch, grow exponentially with position along the undulator z:

$$I_\omega(s, z) \propto \exp(gz).$$

Near the optimal frequency ω_0 at the point s_0 within the bunch, where the longitudinal particle density is maximal, the factor g reaches a maximum and therefore can be represented in the form

$$g \approx \frac{1}{2L_g}[1 - a(\omega - \omega_0)^2 - b(s - s_0)^2],$$

where L_g is the power gain length at the optimal frequency and peak current, and a and b are constants.

The radiated energy W is then proportional to

$$W \propto \int_{-\infty}^{\infty} \int_{-\infty}^{\infty} \int_{2L_g}^{z} |I_\omega(s, z')|^2 \, dz' \, ds \, d\omega$$

$$\propto \int_{-\infty}^{\infty} \int_{-\infty}^{\infty} \int_{2L_g}^{z} \exp\left[\frac{1 - a(\omega - \omega_0)^2 - b(s - s_0)^2}{L_g} z'\right] dz' \, ds \, d\omega \approx \frac{L_g^2}{z} \exp\left(\frac{z}{L_g}\right) \frac{\pi}{\sqrt{ab}}.$$

The results of fitting a function of the form $A(L_g^2/z) \exp(z/L_g)$ with two parameters (A and L_g) at three points (after the second, third, and fourth undulators) are presented in Table II, where W_1 is the measured radiation energy after the first undulator (from the first data points in Fig. 2).

The gain lengths, using the "most probable" values listed in Table I and calculated by Xie's parametrization [20], are 0.9 m and 0.7 m, respectively. The source of discrepancy

between theory and the experimentally measured values is not known; however, it could be due to a number of items. For instance, the uncertainty in the measurements of energy spread and average beta function, in particular, within the undulator, can lead to such a substantial increase in the gain length. Nevertheless, even though the measured gain length was not as short as the beam property measurements appear to indicate, the fact remains that exponential
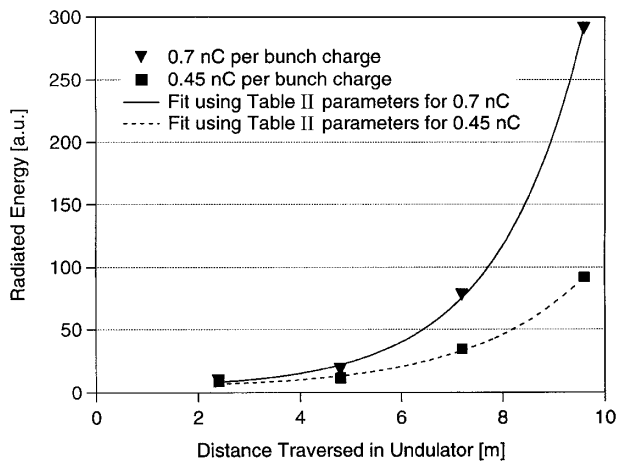
FIG. 2. Radiated energy as a function of distance along the undulator system. The triangles are for 0.7 nC and the squares are for 0.45 nC bunch charge. The solid and dashed lines are the fits using the fitting parameters listed in Table II.

growth of the signal as a function of length along the undulator was seen.

The fitted value for A also gives a similar, albeit rough, agreement with theory. Assuming that the radiation energy W_1 is due mostly to spontaneous emission, one can normalize A to it. The results of our measurements may then be expressed as

$$W \approx 0.18 W_1 \frac{L_g^2}{z} \exp\left(\frac{z}{L_g}\right). \tag{1}$$

A coarse estimate of the energy W radiated per shot is

$$W \approx \frac{K^2[J_0(\frac{K^2}{4+2K^2}) - J_1(\frac{K^2}{4+2K^2})]^2}{1 + K^2/2} \frac{Ne^2}{8\pi\varepsilon\beta} \frac{L_g^2}{z} \exp\left(\frac{z}{L_g}\right), \tag{2}$$

where e is the electron charge, N is the number of particles per bunch, K is the undulator strength parameter, $J_{0,1}$ are Bessel functions, and $\varepsilon\beta$ is the square of the transverse beam size (about 0.02 mm^2). Calculation of A using Eq. (2) gives $A \cong 0.1 W_1$, which is in rough agreement with the measured factor given in Eq. (1).

Angular distribution.—An estimate of the FWHM angular divergence of the SASE radiation is $\sqrt{2\lambda/\pi L_g}$. Using the measured divergence of 0.46 mrad gives $L_g \cong 1.6$ m. This is an independent confirmation of the 1.46 m value (at 0.7 nC) found in the previous section; however, the accuracy of the measured divergence is such that this is only a rough estimate.

In summary, the exponential growth of the optical signal versus the undulator length in the SASE FEL has been explicitly demonstrated at 530 nm. An effective gain length of about 1.5 m was measured in two different ways.

TABLE II. Fit parameters.

Q [nC]	L_g [m]	A	A/Q	A/W_1
0.45	1.82	1.37	3.1	0.17
0.7	1.46	1.84	2.6	0.2

It is not yet possible for us to measure all electron beam properties at the same time that we are measuring the 530-nm signal. This presently prevents us from making an exact one-to-one correspondence between the theory and measured results.

*Corresponding author.
Electronic address: milton@aps.anl.gov
†Present address: Budker Institute of Nuclear Physics, 630090 Novosibirsk, Russian Federation.
‡Present address: Brookhaven National Laboratory, Upton, NY 11973.

[1] Y. S. Derbenev, A. M. Kondratenko, and E. L. Saldin, Nucl. Instrum. Methods Phys. Res. **193**, 415 (1982).
[2] R. Bonifacio, C. Pellegrini, and L. M. Narducci, Opt. Commun. **50**, 6 (1985).
[3] M. Hogan *et al.,* Phys. Rev. Lett. **81**, 4897 (1998).
[4] J. Andruszkow *et al.,* Phys. Rev. Lett. (to be published).
[5] T. J. Orzechowski *et al.,* Nucl. Instrum. Methods Phys. Res., Sect. A **250**, 144 (1986).
[6] R. Tatchyn *et al.,* Nucl. Instrum. Methods Phys. Res., Sect. A **374**, 274 (1996).
[7] M. Cornacchia *et al.,* "Linac Coherent Light Source (LCLS) Design Study Report," Stanford University–University of California Report No. SLAC-R-521/UC-414, revised 1998.
[8] T. Aberg *et al.,* "A VUV Free Electron Laser at the TESLA Test Facility at DESY. Conceptual Design Report," DESY Report No. TESLA-FEL 95-03, 1995.
[9] "Conceptual Design of a 500 GeV e^+e^- Linear Collider with Integrated X-Ray Laser Facility," edited by R. Brinkmann, G. Materlik, J. Rossbach, and A. Wagner, DESY Report No. DESY97-048, 1997.
[10] M. Babzien *et al.,* Phys. Rev. E **57**, 6093 (1998).
[11] S. Biedron *et al.,* in *Proceedings of the 1999 Particle Accelerator Conference* (IEEE, New York, 1999), pp. 2024–2026.
[12] G. Travish, N. Arnold, and R. Koldenhoven, in Proceedings of the Twentieth International Free-Electron Laser Conference, Hamburg (to be published).
[13] S. V. Milton *et al.,* Nucl. Instrum. Methods Phys. Res., Sect. A **407**, 210 (1998).
[14] S. V. Milton *et al.,* Proc. SPIE Int. Soc. Opt. Eng. **3614**, 86 (1999).
[15] I. B. Vasserman *et al.,* in *Proceedings of the 1999 Particle Accelerator Conference* (Ref. [11]), pp. 2489–2491.
[16] I. B. Vasserman, N. A. Vinokurov, and R. J. Dejus, in the 11th National Conference on Synchrotron Radiation Instrumentation, Stanford, CA (to be published).
[17] E. Gluskin *et al.,* Nucl. Instrum. Methods Phys. Res., Sect. A **429**, 358 (1999).
[18] A. Lumpkin *et al.,* Nucl. Instrum. Methods Phys. Res., Sect. A **429**, 336 (1999).
[19] P. Catravas *et al.,* Phys. Rev. Lett. **82**, 5261 (1999).
[20] M. Xie, in *Proceedings of the 1995 Particle Accelerator Conference* (IEEE, Dallas, 1995), pp. 183–185.